Acta Crystallographica Section F
Structural Biology and Crystallization Communications
ISSN 1744-3091

Preliminary neutron crystallographic analysis of selectively CH_3-protonated deuterated rubredoxin from *Pyrococcus furiosus*

K. L. Weiss,[a] F. Meilleur,[b,c] M. P. Blakeley[d] and D. A. A. Myles[a]*

[a]Oak Ridge National Laboratory, Chemical Sciences Division, Center for Structural Molecular Biology, PO Box 2008, Oak Ridge, TN 37831, USA, [b]North Carolina State University, Department of Molecular and Structural Biochemistry, Raleigh, NC 27695, USA, [c]Oak Ridge National Laboratory, Neutron Scattering Sciences Division, PO Box 2008, Oak Ridge, TN 37831, USA, and [d]Institut Laue-Langevin, 6 Rue Jules Horowitz, 38042 Grenoble, France

Correspondence e-mail: mylesda@ornl.gov

Received 1 April 2008
Accepted 9 May 2008

Neutron crystallography is used to locate H atoms in biological materials and can distinguish between negatively scattering hydrogen-substituted and positively scattering deuterium-substituted positions in isomorphous neutron structures. Recently, Hauptman & Langs (2003; *Acta Cryst.* A**59**, 250–254) have shown that neutron diffraction data can be used to solve macromolecular structures by direct methods and that solution is aided by the presence of negatively scattering H atoms in the structure. Selective-labeling protocols allow the design and production of H/D-labeled macromolecular structures in which the ratio of H to D atoms can be precisely controlled. Methyl selective-labeling protocols were applied to introduce (^{1}H-δ methyl)-leucine and (^{1}H-γ methyl)-valine into deuterated rubredoxin from *Pyrococcus furiosus* (PfRd). Here, the production, crystallization and preliminary neutron analysis of a selectively CH_3-protonated deuterated PfRd sample, which provided a high-quality neutron data set that extended to 1.75 Å resolution using the new LADI-III instrument at the Institut Laue-Langevin, are reported. Preliminary analysis of neutron density maps allows unambiguous assignment of the positions of H atoms at the methyl groups of the valine and leucine residues in the otherwise deuterated rubredoxin structure.

1. Introduction

Neutron protein crystallography is highly sensitive to the location of H atoms in biological macromolecules and has been used to determine H-atom positions, protonation states and solvent water in a number of protein structures in which these could not be reliably determined from X-ray crystal structures alone. H and/or D atoms are more readily located and distinguished in a neutron analysis because the neutron scattering lengths of hydrogen, $b_n = -0.374 \times 10^{-12}$ cm, and deuterium, $b_n = +0.667 \times 10^{-12}$ cm, are comparable to those of other biological atoms. The difference in magnitude and phase between the hydrogen and deuterium isotopes allows the use of neutron diffraction to determine the pattern and extent of H (or ^{1}H)/D (or ^{2}H) isotope substitution in neutron crystal structures, in which the negative density features that arise from H atoms are readily distinguished from the positive density of D atoms. This has been used in H/D-exchange experiments to provide insight into the solvent accessibility of individual amino acids, the mobility and flexibility of interesting domains and the exchange dynamics (Kossiakoff, 1985). The ability to discriminate between H and D atoms in isomorphous neutron structures is also of interest in the solution of macromolecular structures using direct methods. Recently, Hauptman & Langs (2003) reported the development of a new neutron *Shake-and-Bake* (*SnB*) protocol that was used to solve the structure of cyclosporin A, where they found that the native structure with negative H scattering was much easier to solve than the D isomorph for which all atoms should appear as positive peaks in the neutron density map. Such approaches may allow the solution of small or recalcitrant protein, polypeptide or nucleic acid structures that are difficult to phase by classical techniques. The extension of this approach to the solution of macromolecular systems is likely to be greatly aided by the design and production of H/D-labeled macro-

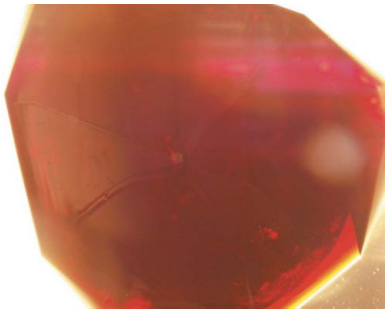

molecular structures in which the ratio of H to D atoms can be precisely controlled. Here, we describe the application of a selective labeling protocol and the first experimental neutron data collection from the small iron–sulfur redox protein rubredoxin from *Pyrococcus furiosus* (PfRd).

The anaerobic archaebacteria *P. furiosus*, which was isolated from volcanic marine vents, grows optimally at 373 K (Fiala & Stetter, 1986) and produces an extremely stable form of rubredoxin with a melting temperature of around 473 K (Hiller *et al.*, 1997). The biological function of rubredoxin is likely to involve electron-transfer processes, but has not yet been determined. Structurally, PfRd contains 53 amino acids and one iron bound by the S atoms of four cysteine residues (Day *et al.*, 1992). With only 413 C/N/O/S atoms and 387 H atoms, rubredoxin represents a reasonable model system for the initial development of *ab initio* phasing techniques using neutron data alone. The preparation and analysis of perdeuterated PfRd will be published elsewhere. In order to limit the number of labels and thus aid analysis, hydrogen labels were introduced at just four residues, Leu32/Leu51 and Val4/Val37, using a well known selective protonation strategy to selectively label deuterated rubredoxin with (^{1}H-δ methyl)-leucine and (^{1}H-γ methyl)-valine by utilizing the precursor (3-^{2}H) α-ketoisovalerate (Goto *et al.*, 1999). Here, we report the production, crystallization and preliminary neutron crystallographic analysis of the selectively CH_3-protonated deuterated sample, which provided a high-quality neutron data set extending to 1.75 Å resolution.

2. Experimental procedures

2.1. Expression and purification of CH_3-protonated deuterated rubredoxin from *P. furiosus*

Escherichia coli BL21 (DE3) cells were transformed with a pET24d expression vector carrying the gene encoding PfRd, which was a generous gift from Michael Adams and Frank Jenney at the University of Georgia. Kanamycin selection (50 mg l^{-1}) was used in all cultures. Prior to protein expression, a single colony of transformants were grown on LB agar and then transferred to hydrogenated minimal medium agar containing 0.5%(*w*/*v*) glycerol. The minimal medium was prepared as described previously (Meilleur *et al.*, 2004) except that the $FeCl_3$ concentration was doubled and $ZnSO_4$ was excluded in order to avoid the expression of zinc-substituted rubredoxin (Eidsness *et al.*, 1997; Jenney & Adams, 2001).

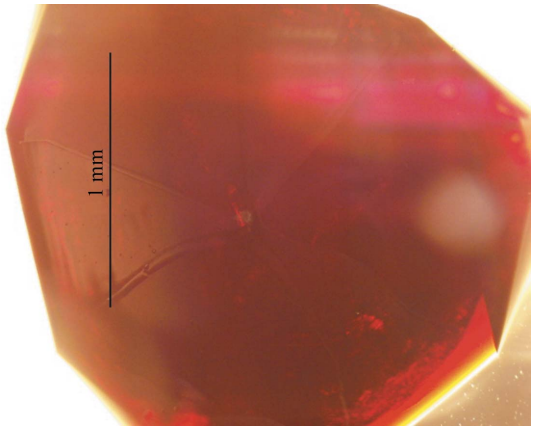

Figure 1
Selectively CH_3-labeled deuterated rubredoxin crystals grown by vapour-diffusion and microseeding techniques. The approximate crystal volume is 4.1 mm^3.

After growth on hydrogenated minimal medium agar, cells were adapted to deuterated minimal medium agar and then liquid deuterated minimal medium. The deuterated medium was prepared in the same manner as the hydrogenated medium using D_2O and 0.5%(*w*/*v*) d_8-glycerol. Salts containing labile H atoms were exchanged by two D_2O dissolution–evaporation cycles utilizing a rotary evaporator. (3-^{2}H) α-ketoisovalerate was prepared by warming a 25 m*M* solution of α-ketoisovalerate in D_2O at pH 12.5 and 318 K for 3 h (Goto *et al.*, 1999). The resulting solution was acidified with 35% DCl to pH 7.5 and sterile-filtered prior to use. After three cycles of adaptation in liquid deuterated medium, two 1 l cultures utilizing 0.3%(*w*/*v*) perdeuterated D-glucose as a carbon source were inoculated and cultured at 310 K. The growth rate of the cultures was carefully monitored by measurement of the optical density at 600 nm (OD_{600}). 1 h prior to induction, 100 mg (3-^{2}H) α-ketoisovalerate was added to each 1 l culture. After the cultures reached an OD_{600} of 0.9, expression was induced with 1 m*M* IPTG for 4 h. Cells were harvested *via* centrifugation, flash-frozen and stored at 193 K prior to purification. Selectively CH_3-protonated deuterated rubredoxin was purified using a combination of heat treatment, anion-exchange chromatography and gel filtration as described elsewhere (Jenney & Adams, 2001). It should be noted that a HiTrap Q HP column (GE Healthcare) was utilized for the anion-exchange step instead of Fast Flow DEAE-Sepharose and further purification to separate the three N-terminal forms of PfRd was not carried out. The rubredoxin-containing fractions were characterized by their UV–visible absorption spectra and their concentrations were determined by absorbance at 494 nm ($\varepsilon_{494\,\mathrm{nm}} = 9.22$ mM^{-1} cm^{-1}). Fractions with an absorbance ratio (494/280 nm) of greater than 0.35 were combined and concentrated to 40 mg ml^{-1}. Three dilution–concentration cycles using a 1:10 dilution ratio were performed to exchange the hydrogenated gel-filtration buffer to 99% D_2O.

2.2. Crystallization and data collection

Crystallization was carried out by vapor diffusion at room temperature using seeding conditions that were re-optimized from the published conditions (Bau *et al.*, 1998). Salt solutions were prepared in D_2O after exchanging salt hydrogen to deuterium by rotary evaporation. Crystal clusters were obtained overnight by the hanging-drop method using a reservoir consisting of 3.8 *M* sodium/potassium phosphate (0.3:0.7 molar ratio NaH_2PO_4:K_2HPO_4) and sample drops composed of 1 µl protein solution (40 mg ml^{-1} in D_2O) mixed with 1 µl reservoir solution. Clusters were crushed to micro-seed 2 µl hanging drops containing 1 µl 18–20 mg ml^{-1} protein solution and 1 µl reservoir solution pre-equilibrated against 3.8–4.0 *M* sodium/potassium phosphate (equimolar ratio). Small prismatic crystals grew in a few hours. Crystals suitable for neutron diffraction (Fig. 1) were obtained by macro-seeding 20 µl sitting drops containing 18–20 mg ml^{-1} protein and 3.0 *M* sodium/potassium phosphate and equilibrated against 3.4 *M* sodium/potassium phosphate.

2.3. Structure determination and model refinement

A crystal with dimensions of 2.5 × 1.5 × 1.1 mm (volume 4.1 mm^3) was mounted in a 3 mm diameter quartz capillary. Crystal hydration was maintained with reservoirs of sodium/potassium phosphate solution placed at both capillary ends. Wax was used for sealing. Neutron quasi-Laue data were collected at 293 K on the recently commissioned LADI-3 beamline (Blakeley, personal communication) installed on end-station T17 of cold neutron guide H142 at ILL. A Ni/Ti multilayer wavelength selector was used to select a narrow

wavelength bandpass ($\Delta\lambda/\lambda \simeq 25\%$; Myles *et al.*, 1997). The data set collected for the selectively CH_3-protonated deuterated rubredoxin was composed of 20 images of 4 h exposure each, with a φ-step separation of 5° between images. A typical quasi-Laue neutron diffraction pattern is shown in Fig. 2.

The neutron Laue data were processed using the Daresbury Laboratory software *LAUEGEN* modified to account for the cylindrical geometry of the detector (Campbell *et al.*, 1998). The program *LSCALE* (Arzt *et al.*, 1999) was used to derive the wavelength-normalization curve using the intensity of symmetry-equivalent reflections measured at different wavelengths. The data were then scaled and merged using *SCALA* (Collaborative Computational Project, Number 4, 1994). Data-reduction statistics are summarized in Table 1.

Table 1
Data-reduction statistics.

Values in parentheses are for the highest resolution shell.

Source	LADI-III, Institut Laue-Langevin
Settings	20
Space group	$P2_12_12_1$
Unit-cell parameters (Å, °)	a = 34.1, b = 34.9, c = 43.7
Resolution	27.2–1.65 (1.74–1.65)
No. of reflections (measured/unique)	27322/4602
Redundancy	5.9 (1.9)
Completeness (%)	71.6 (33.6)
$R_{\rm merge}$	0.092 (0.108)
Wavelength range (Å)	3.1–4.2
Mean $I/\sigma(I)$	16.0 (5.2)

3. Results and discussion

3.1. Selectively CH_3-labeled deuterated rubredoxin

Deuterated rubredoxin selectively labeled with (^{1}H-δ methyl)-leucine and (^{1}H-γ methyl)-valine was expressed, yielding 3 g of wet cell paste per litre of flask culture. Protein-expression levels and purity were assessed by SDS–PAGE and the $A_{494\,\rm nm}/A_{280\,\rm nm}$ ratio (data not shown). The yield of selectively CH_3-labeled deuterated rubredoxin was approximately 10 mg per gram of wet cell paste. Crystallization conditions were readily re-optimized from the published conditions, showing that deuteration of the protein did not affect crystallization behaviour significantly. Large brick-shaped crystals (up to 4.5 mm^3 in volume) were obtained in just 48 h (Fig. 1).

3.2. Preliminary neutron structure analysis

The statistics in Table 1 show, as expected, that the neutron diffraction data from this highly deuterated rubredoxin crystal are of higher quality than data recorded from fully hydrogenated structures (for a review, see Myles, 2006). The data recorded in the highest 1.74–1.65 Å resolution shell remain strong [$I/\sigma(I) \simeq 5.2$], although the completeness is low (33.6%). This suggests that the resolution limit of diffraction is set by the instrument configuration and neutron wavelength (3.2–4.2 Å) range used rather than by the sample. The resolution may be extended by tuning the instrument to neutrons of shorter wavelength. We have restricted the data to 1.75 Å for initial refinement (completeness of ∼50%).

Preliminary structure refinement was performed using *CNSsolve* (Brünger *et al.*, 1998) starting from a high-resolution X-ray structure of hydrogenated wild-type PfRd (PDB code 1brf; Bau *et al.*, 1998), omitting all water molecules. D atoms were generated from the starting X-ray model using the topology and parameter files

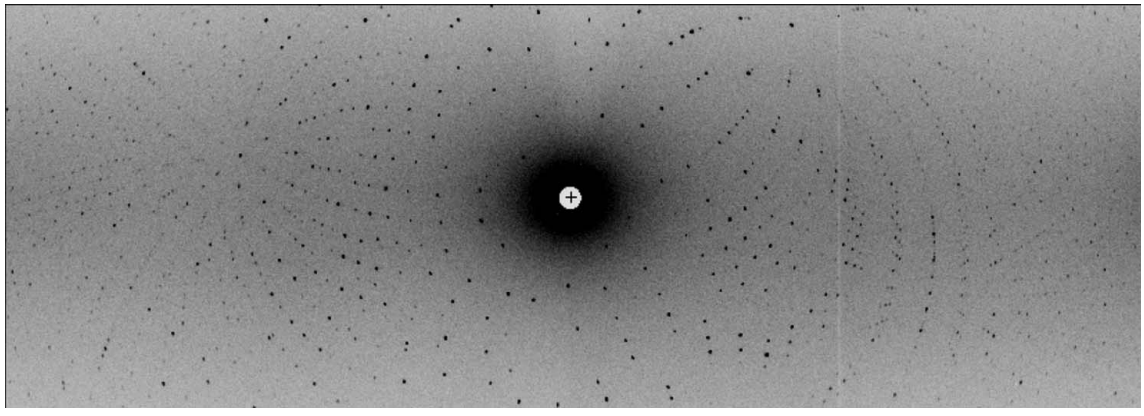

Figure 2
A quasi-Laue neutron diffraction image from CH_3-labeled deuterated rubredoxin collected in 4 h on the LADI-III beamline at the Institut Laue-Langevin.

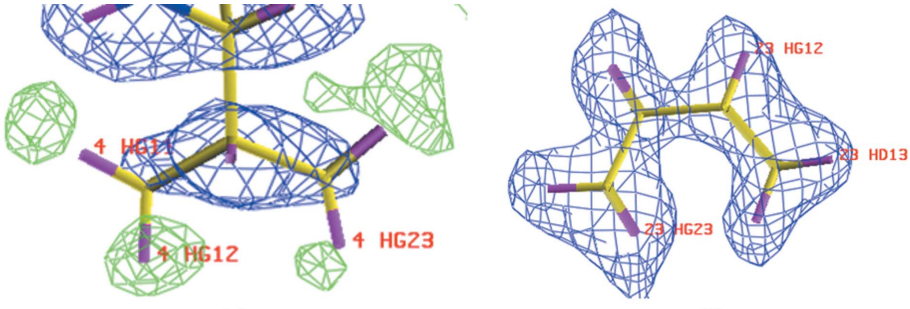

(*a*) (*b*)

Figure 3
Preliminary neutron density maps of selectively CH_3-labeled deuterated rubredoxin: (*a*) residue Val4, showing strong negative neutron density (green) at the position of the selectively hydrogen-labeled methyl groups; (*b*) residue Ile23, showing strong positive neutron density (blue) at the position of deuterated methyl groups.

protein-allhdg.top and protein-allhdg.param from the *CNS* package specific to NMR refinement (Brünger *et al.*, 1998), with the exception of the side chains of Ala, Val, Leu and Ile. Appropriate neutron-scattering lengths were used throughout all subsequent refinement steps (*International Tables for Crystallography*, 1995, Vol. *C*, pp. 384–391). Rigid-body refinement was performed against all neutron data to 1.75 Å, followed by minimization of all atom positions and *B*-factor refinement. Neutron density maps ($2F_o - F_c$ and $F_o - F_c$) were calculated and the side chains of Ala, Leu, Val and Ile were carefully examined using the program *O* (Jones *et al.*, 1991) to discriminate negative hydrogen neutron density peaks from positive deuterium neutron density peaks. These preliminary maps show that Ala and Ile have strong positive peaks indicating that they are deuterated (Fig. 3*a*) and that Leu and Val have strong negative peaks indicating that they are hydrogenated (Fig. 3*b*). In addition, Fig. 3 emphasizes a more general benefit of using deuterium-labeled protein in neutron crystallography, since the cancellation of density observed between the negatively scattering H atoms and positively scattering C atoms in Fig. 3(*a*) is avoided completely when the protein residues are deuterated (Fig. 3*b*). In order to complete refinement of CH_3-labeled deuterated rubredoxin, a high-resolution (1.25 Å) room-temperature X-ray data set has been collected (SER-CAT, APS). A joint structure refinement of the X-ray and neutron diffraction data is in progress.

4. Conclusions

This is the first reported use of selective H/D labeling for neutron protein crystallography. The aim of this work was to demonstrate the design and control of hydrogen incorporation in an otherwise deuterated protein structure and to provide experimental neutron data for structure solution by direct methods (to be reported elsewhere). The high quality of the neutron data has allowed unambiguous assignment of the H-atom positions at the CH_3 groups of Val and Leu residues. These hydrogenated positions are readily distinguished from the deuterated CD_3 groups of Ala and Ile in the remainder of this otherwise deuterated rubredoxin structure. Other expression systems and labeling schemes are now under development that will allow the introduction of labels tailored to specific applications that may extend beyond crystallography. For example, small-angle neutron scattering (Laux *et al.*, 2008), reflectometry and neutron spectroscopy can all benefit from selective labeling.

This research was sponsored by the Laboratory Directed Research and Development Program of Oak Ridge National Laboratory, managed by UT-Battelle LLC for the US Department of Energy. This research was performed in association with a Human Frontier Science Program award to Professor Herbert Hauptman. We gratefully acknowledge the gift of the *P. furiosus* rubredoxin clone from F. E. Jenney and M. W. W. Adams (University of Georgia).

References

Arzt, S., Campbell, J. W., Harding, M. M., Hao, Q. & Helliwell, J. R. (1999). *J. Appl. Cryst.* **32**, 554–562.
Bau, R., Rees, D. C., Kurtz, D. M., Scott, R. A., Huang, H. S., Adams, M. W. W. & Eidsness, M. K. (1998). *J. Biol. Inorg. Chem.* **3**, 484–493.
Brünger, A. T., Adams, P. D., Clore, G. M., DeLano, W. L., Gros, P., Grosse-Kunstleve, R. W., Jiang, J.-S., Kuszewski, J., Nilges, M., Pannu, N. S., Read, R. J., Rice, L. M., Simonson, T. & Warren, G. L. (1998). *Acta Cryst.* D**54**, 905–921.
Campbell, J. W., Hao, Q., Harding, M. M., Nguti, N. D. & Wilkinson, C. (1998). *J. Appl. Cryst.* **31**, 496–502.
Collaborative Computational Project, Number 4 (1994). *Acta Cryst.* D**50**, 760–763.
Day, M. W., Hsu, B. T., Joshua-Tor, L., Park, J. B., Zhou, Z. H., Adams, M. W. W. & Rees, D. C. (1992). *Protein Sci.* **1**, 1494–1507.
Eidsness, M. K., Richie, K. A., Burden, A. E., Kurtz, D. M. Jr & Scott, R. A. (1997). *Biochemistry*, **36**, 10406–10413.
Fiala, G. & Stetter, K. O. (1986). *Arch. Microbiol.* **145**, 56–61.
Goto, N. K., Gardner, K. H., Mueller, G. A., Willis, R. C. & Kay, L. E. (1999). *J. Biomol. NMR*, **13**, 369–374.
Hauptman, H. A. & Langs, D. A. (2003). *Acta Cryst.* A**59**, 250–254.
Hiller, R., Zhou, Z. H., Adams, M. W. W. & Englander, S. W. (1997). *Proc. Natl Acad. Sci. USA*, **94**, 11329–11332.
Jenney, F. E. Jr & Adams, M. W. W. (2001). *Methods Enzymol.* **334**, 45–55.
Jones, T. A., Zou, J.-Y., Cowan, S. W. & Kjeldgaard, M. (1991). *Acta Cryst.* A**47**, 110–119.
Kossiakoff, A. A. (1985). *Annu. Rev. Biochem.* **54**, 1195–1227.
Laux, V., Callow, P., Svergun, D. I., Timmins, P. A., Forsyth, V. T. & Haertlein, M. (2008). *Eur. Biophys. J.* doi:10.1007/s00249-008-0280-5.
Meilleur, F., Contzen, J., Myles, D. A. A. & Jung, C. (2004). *Biochemistry*, **43**, 8744–8753.
Myles, D. A. A. (2006). *Curr. Opin. Struct. Biol.* **16**, 630–637.
Myles, D. A. A., Bon, C., Langan, P., Cipriani, F., Castagna, J. C., Lehmann, M. S. & Wilkinson, C. (1997). *Physica B*, **241–243**, 1122–1130.